

# Non-thermal X-ray Emission from Supernova Remnants

Jacco Vink

*SRON National Institute for Space Research, Sorbonnelaan 2, 3584CA, Utrecht, The Netherlands*

**Abstract.** Recent studies of narrow, X-ray synchrotron radiating filaments surrounding young supernova remnants indicate that magnetic fields strengths are relatively high,  $B \sim 0.1$  mG, or even higher, and that diffusion is close to the Bohm limit. I illustrate this using Cas A as an example. Also older remnants such as RCW 86 appear to emit X-ray synchrotron radiation, but the emission is more diffuse, and not always confined to a region close to the shock front. I argue that for RCW 86 the magnetic field is likely to be low ( $B \approx 17 \mu\text{G}$ ), and at the location where the shell emits X-ray synchrotron radiation the shock velocity is much higher than the average shock velocity of  $\sim 600 \text{ km s}^{-1}$ .

## INTRODUCTION

Supernova remnants (SNRs) are believed to be the dominant source of Galactic cosmic rays, at least for energies up to  $3 \times 10^{15}$  eV, corresponding to the “knee” in the cosmic ray spectrum, and possibly even up to  $10^{19}$  eV, the “ankle” [1]. However, until a decade ago the best direct evidence for cosmic ray acceleration by SNR shocks consisted of radio synchrotron radiation from shell-type<sup>1</sup> SNRs, providing evidence for the presence of accelerated electrons with energies in the GeV range, far short of the “knee” energy, and not providing any evidence for the acceleration of nuclei, which dominate the cosmic ray spectrum.

Recent progress has been made due to major advances in two fields of high energy astrophysics. One is the development of atmospheric Cerenkov detectors, which are now capable of imaging TeV  $\gamma$ -rays arcminute resolution, as shown by the new, exciting image of the SNR RX J1713.7-3946 obtained by the High Energy Stereoscopic System (*H.E.S.S.*). The other progress is in the field of X-ray astronomy, and in particular the emergence of imaging spectroscopy with CCD detectors. The first satellite mission employing these detectors was *ASCA*, but with *Chandra* imaging spectroscopy is now possible at the sub-arcsecond level. Imaging spectroscopy with *ASCA* facilitated the first discovery of X-ray synchrotron radiation from a shell-type SNR, SN 1006, as it allowed for the spatial separation of X-ray line emission from pure continuum emission [2].

The detection of X-ray synchrotron radiation from SNRs provides direct evidence for electron acceleration up to energies of 10-100 TeV. Although it does not per se

---

<sup>1</sup> I single out shell-type SNRs, as the radiation from those remnants are not dominated by synchrotron radiation from particles accelerated by the pulsar magnetosphere.

proof the acceleration of cosmic ray nuclei by SNRs, and the electron energies fall short of the “knee” energy, it does prove that SNRs are capable of efficient particle acceleration. Moreover, the combination of X-ray synchrotron and TeV  $\gamma$ -ray radiation puts constraints on the relative contributions of several  $\gamma$ -ray radiation mechanisms, i.e.  $\pi^0$ -decay, bremsstrahlung or inverse Compton emission, as was done for RX J1713.7-3946 (G347.3-0.5) or Cas A [3, 4, 5]. This is of considerable interest as an unambiguous detection of  $\pi^0$ -decay would be direct evidence for the acceleration of nuclei.

Finally, the morphology of X-ray synchrotron radiating filaments in young supernova remnants gives new insights in the acceleration properties of SNR shock fronts, e.g. in relation to the idea that cosmic ray streaming leads to significant magnetic field amplification near high Mach number shocks due to non-linear growth of plasma waves [6]. I will discuss this topic using the youngest known Galactic SNR, Cas A, as an example.

Although, it may not be surprising that young SNRs can efficiently accelerate electrons up to 10 TeV, it is surprising that some apparently older remnants also appear to be X-ray synchrotron sources. Moreover, the non-thermal X-ray emission from these remnants is more diffuse and not confined to narrow regions close to the shock front. Examples are RCW 86 [7, 8, 9], RX J1713.7-3946<sup>2</sup> [3, 10], and even the superbubble 30 Dor C [11, 12]. As these remnants have slower shock velocities, which implies a lower acceleration rate, one would expect that synchrotron losses would prevent synchrotron radiation to occur in the X-ray band. In this context I will present some preliminary results of *XMM-Newton* and *Chandra* observations of RCW 86.

## COSMIC RAY ACCELERATION AT CAS A’S FAST SHOCKS

Cas A is the brightest radio source in the sky and has been for a long time the archetypal young shell-type SNR. The supernova event may have been dim, as there are no historical records of a bright supernova near the approximate year of explosion AD 1671 [13, 14]. The estimate for the explosion date is based on the kinematics of fast moving optical knots. However, a more reliable estimate of the current shock velocity comes from X-ray expansion measurements, which give a shock velocity of  $\sim 5000 \text{ km s}^{-1}$  [15, 16]. The distance to Cas A is 3.4 kpc [17].

The first evidence for non-thermal X-ray emission was the detection of hard X-ray emission above 10 keV by several instruments [18, 19, 20], but it is still debated whether the non-thermal, hard X-ray emission is indeed synchrotron radiation [21, 5] (see below).

However, the high spatial resolution images by *Chandra* reveal thin filaments surrounding Cas A, which are especially prominent in images extracted in the 4-6 keV continuum dominated band (Fig. 1). These filaments mark the onset of radio emission [22], which is a clear indication that the X-ray emission is coming from a region close to the shock front. The spectra of these filaments show a lack of line emission compared to neighboring regions, an indication for a synchrotron emission component [5].

---

<sup>2</sup> The age and shock velocity of RX J1713.7-3946 is highly uncertain.

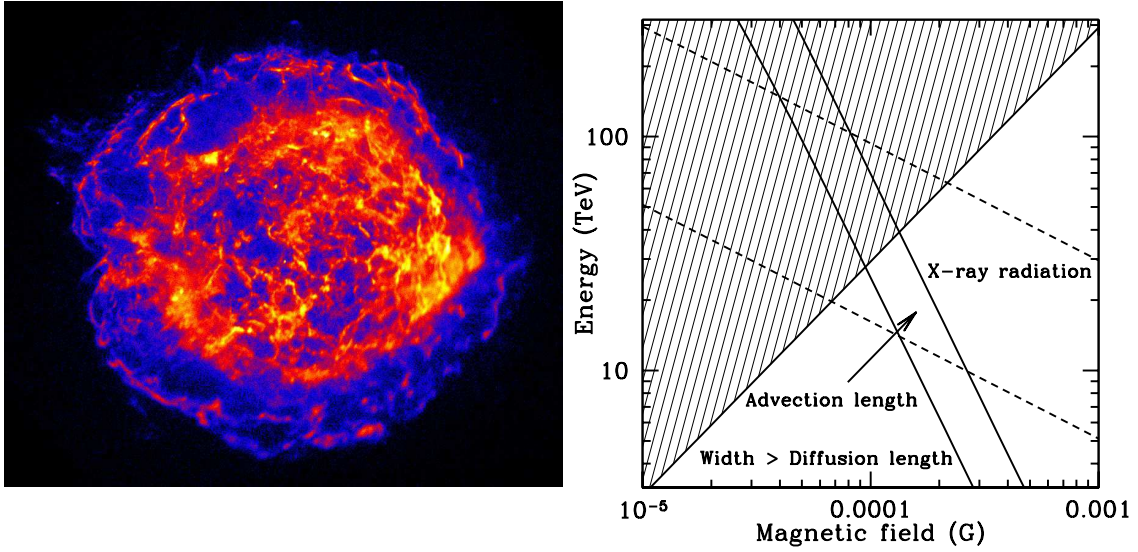


**FIGURE 1.** A recent *Chandra* image [23] in the 4-6 keV continuum band, intensities have been logarithmically scaled (left). Note the thin filaments marking the border of the remnant (NB the point spread function is not uniform). The remnant has a radius of about  $2.5'$ . Right: Determination of the maximum electron energy versus magnetic field strength for the region just downstream of Cas A's shock front, as determined from the thickness of the filaments. The shaded area is excluded as the filament width cannot be smaller than the diffusion length [c.f. 5].

The importance of these filaments is that their widths can be used to estimate simultaneously the downstream magnetic field strength and the electron energy [5, 24]. The reason is that as the plasma moves away from the shock front with a velocity  $u = \frac{1}{\chi} V_s$ , the high energy electrons suffer synchrotron losses on a time scale  $\tau_{loss} = 635/B^2 E$  s ( $V_s$  is the shock velocity and  $\chi$  the shock compression ratio). As a result, the highest energy electrons can only be found in a region confined to a layer with a thickness corresponding to the advection length scale:

$$l_a = u\tau_{loss}. \quad (1)$$

On the other hand the photon energy for synchrotron radiation is:

$$\varepsilon = 7.4 E^2 B \text{ keV}. \quad (2)$$

Using the observed thickness of the filaments,  $1.5''$  to  $4''$ , and assuming a shock compression of  $\chi = 4$ , one can use the above expression to show that the magnetic field strength is  $B \sim 0.1$  mG, and the maximum electron energy  $\sim 10 - 40$  TeV [5]. This is graphically shown in Fig. 1.

This result is interesting, because it establishes that the downstream magnetic field is much higher than the compressed mean Galactic Field,  $B_{Gal} \sim 3 \mu\text{G}$ , and either suggests that the magnetic field surrounding Cas A is high, or that indeed Cosmic Ray streaming has enhanced the magnetic field [6].

In fact, it has now been established that all young supernova remnants, SN 1006, Tycho's, and Kepler's SNR have thin non-thermal X-ray filaments, indicating similarly

high magnetic fields [25, 26, 27]. As it is hard to believe that the magnetic field is high in all young Galactic SNRs, this is evidence for cosmic ray induced magnetic field amplification.

Shortly after the publication of the measurement of Cas A's magnetic field, a different method to estimate the magnetic field near the shock front of SN 1006 was published [28]. Instead of the advection length the diffusion length was used for the length scale defining the widths of the filaments. A similar method was also used by Berezhko et al. for both SN 1006 and Cas A [29, 24]. They argue that, due to projection effects, the actual widths are even smaller than the observed widths, and as a consequence  $B \sim 0.5$  mG for Cas A.

Projection effects may, indeed, be important, but one should be cautious, since for this study Cas A's brightest filaments were selected, and it may be that the filaments are only locally very bright, in which case a spherical shell model may not be appropriate. For SN 1006 there is evidence that the non-thermal emission is not axi-symmetric, but confined to two polar caps [30, 31].

Concerning whether the diffusion or the advection model is right. The distinction for loss limited electron spectra is actually not relevant, they give the same results. I have illustrated this in Fig. 1, where the shaded area shows the values of electron energy and B-field that are excluded, based on the fact that the filament width should be equal to, or larger than the diffusion length,  $l_d$ . I have assumed here Bohm diffusion:

$$l_d = \frac{\kappa}{u} = \frac{1}{3} \frac{cE}{eB} \frac{1}{u}, \quad (3)$$

with  $\kappa$  the diffusion coefficient. That is, the boundary of the region is formed by the diffusion length scale, and this gives a solution almost identical to using the advection length scale  $l_a$  (eq. 1). This is apparently not only true for Cas A but for all young remnants<sup>3</sup>, i.e. it looks like  $l_a \approx l_d$ . Figure 1 does not take into account projection effects, but still indicates a slightly higher magnetic field of  $B = 0.2$  mG and  $E = 25$  TeV.

It is not difficult to see as to why  $l_a \approx l_d$  in the framework of first order Fermi acceleration. First of all note that the acceleration time,  $\tau_{acc}$ , is approximately

$$\tau_{acc} = \frac{\kappa}{u^2}. \quad (4)$$

For efficient acceleration  $\tau_{acc} < \tau_{loss}$ , i.e. (eq. 1,4)

$$\frac{\kappa}{u^2} < \frac{l_a}{u} \iff \frac{\kappa}{u} = l_d < l_a. \quad (5)$$

In other words the advection length scale has to be larger than the diffusion length scale. As soon as for a given energy  $l_d \approx l_a$ , efficient acceleration stops, and the electron spectrum will be cut off, resulting in a steepened photon spectrum around the corresponding photon energy. This is in agreement with the X-ray spectrum, as the observed spectral energy index is  $-2$ , steeper than the radio spectral index of  $-0.78$ .

---

<sup>3</sup> As shown by Dr. J. Ballet at the COSPAR 2004 convention in Paris.

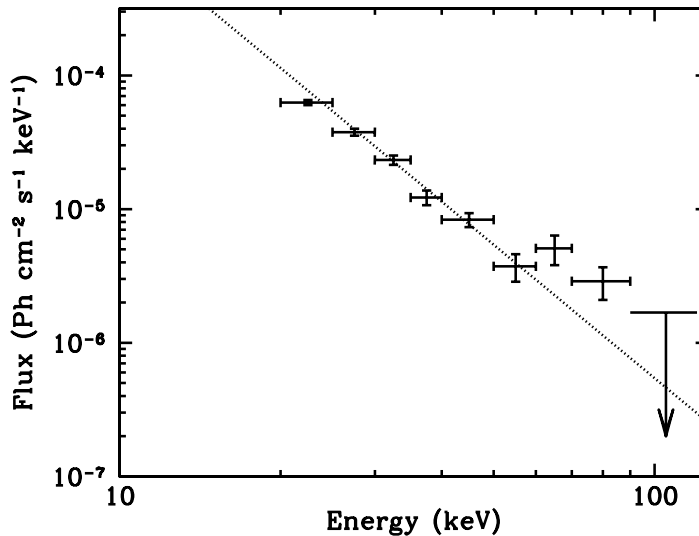


**FIGURE 2.** A hard X-ray spectrum of Cas A as recently observed with the *INTEGRAL*-IBIS instrument (Vink et al. in preparation). The dotted line indicates the best fit power law spectrum as previously determined using *BeppoSAX* data [33]. The excess around 75 keV is due to line emission caused by the decay of  $^{44}\text{Ti}$  [33].

This result has some interesting consequences. First of all, note that the steep spectral index in combination with the observation that  $l_a \approx l_d$ , is additional proof for the correctness of the explanation of the X-ray synchrotron filaments. Secondly, we find  $l_a \approx l_d$  using the approximation of Bohm diffusion. Without Bohm diffusion we would find  $l_d > l_a$ , in violation of (5). The observations therefore, support the idea that the diffusion is near or at the Bohm diffusion limit ( $\delta B/B \sim 1$ ) [c.f. 32], as is expected for non-linear magnetic field amplification. And thirdly, the electron spectrum is apparently loss limited, and not age limited. For an age limited spectrum the maximum energy for the electrons should be similar to that of the proton energy, but for a loss limited spectrum the nuclei can obtain higher energies. Using the shock properties of Cas A and  $B = 0.2$  mG, the maximum energy for nuclei can be  $E_{max} \sim 2 \times 10^{15} Z$  eV, close to the “knee”. Note, however, that the magnetic field may have been higher in the past.

## THE NATURE OF CAS A’S HARD X-RAY EMISSION

One of the first arguments in favor of X-ray synchrotron radiation from Cas A was the existence of non-thermal, hard X-ray emission [18, 20, 19] (Fig. 2). However, the non-thermal rims observed by *Chandra* are likely to contribute only a fraction of 10% to the total flux.

Unfortunately, imaging above 15 keV is extremely difficult, and our knowledge of where the hard X-ray emission predominantly comes from is based on the highest energies that can be imaged with *BeppoSAX* and *XMM-Newton*, i.e. the 8-15 keV energy band [34, 21]. These images, however, suggest that the hard X-ray emission is associated

with the shell of Cas A and peaks in the West [34, 21]. This is also the location of a number of continuum dominated filaments seen by *Chandra* [e.g. 35].

One could of course explain this by assuming that the filaments are similar to the filaments at the edge of Cas A, but projected onto the interior. There are, however, problems with that. First of all, the outside filaments probably just look like filaments due to strong limb brightening. The other argument is that *Chandra* proper motion studies indicate that the kinematics of the interior filaments are systematically different from the kinematics of the outer filaments [36]. The latter have a dynamical timescale of  $\sim 500$  yr, whereas the interior filaments have a timescale similar to the radio knots, i.e.  $> 800$  yr [37].

So what can explain both the presence of the interior filaments, and the hard X-ray spectrum? One problem with X-ray synchrotron radiation is the extremely short life time of the electrons responsible for it: assuming for the interior  $B \sim 1$  mG,  $\tau_{loss} \sim 2$  yr. This would require (re)acceleration in the interior of the remnant. Another problem is that the spectral slope seems to remain constant at  $\Gamma = 3.3$ , from 6-60 keV, whereas X-ray synchrotron radiation is expected to have gradually steepen.

An explanation may be that the hard X-ray emission is due to non-thermal bremsstrahlung from supra-thermal electrons with energies up to 100 keV. A possible model is electron acceleration by lower hybrid waves [38, 39], which predicts the correct spectral slope [5]. However, some of the filaments seem to lack line emission [35], which is a problem for non-thermal bremsstrahlung models.

One way to reconcile the idea of X-ray synchrotron radiation with the high interior magnetic field strength is to invoke those high magnetic fields. It is likely that Cas A's bright radio ring is associated with the contact discontinuity between swept up matter and ejecta. The contact discontinuity is predicted to have a high density, and the magnetic fields may be enhanced due to Rayleigh-Taylor instabilities. It is not unreasonable to suppose that electrons diffusing from a low magnetic field region into the high field region near the contact discontinuity flare up [40].

In fact, electrons entering the high magnetic field will gain energy due to the betatron effect [e.g. 41]. As an example, assume that the the plateau of Cas A has a magnetic field of 0.5 mG, whereas certain regions have magnetic fields as high of 2 mG [42]. If the electrons have been accelerated 100 yr ago, the maximum energy they can have is  $\sim 5$  erg, having a peak emission at 37 eV. As the electrons enter the 2 mG region the betatron mechanism can increase the energy by maximally a factor 2. The peak radiation energy, however, can increase by a factor 16 (see eq. 2). This does require that the electrons diffuse rapidly: a 10 erg electron in a 2 mG field has a half energy life of 6 months.

Diffusion of electrons into high magnetic field regions may explain why the X-ray filaments seem to mark the edges of bright radio regions [36]: the highest energy electrons cannot penetrate the high magnetic field regions too deeply without losing a substantial part of their energy. Moreover, the non-thermal emission may be more pronounced in the West, as the bright ring appears closer to the shock front. In other words, the electrons may have been accelerated more recently, and as a consequence they start with a higher energy in the first place.

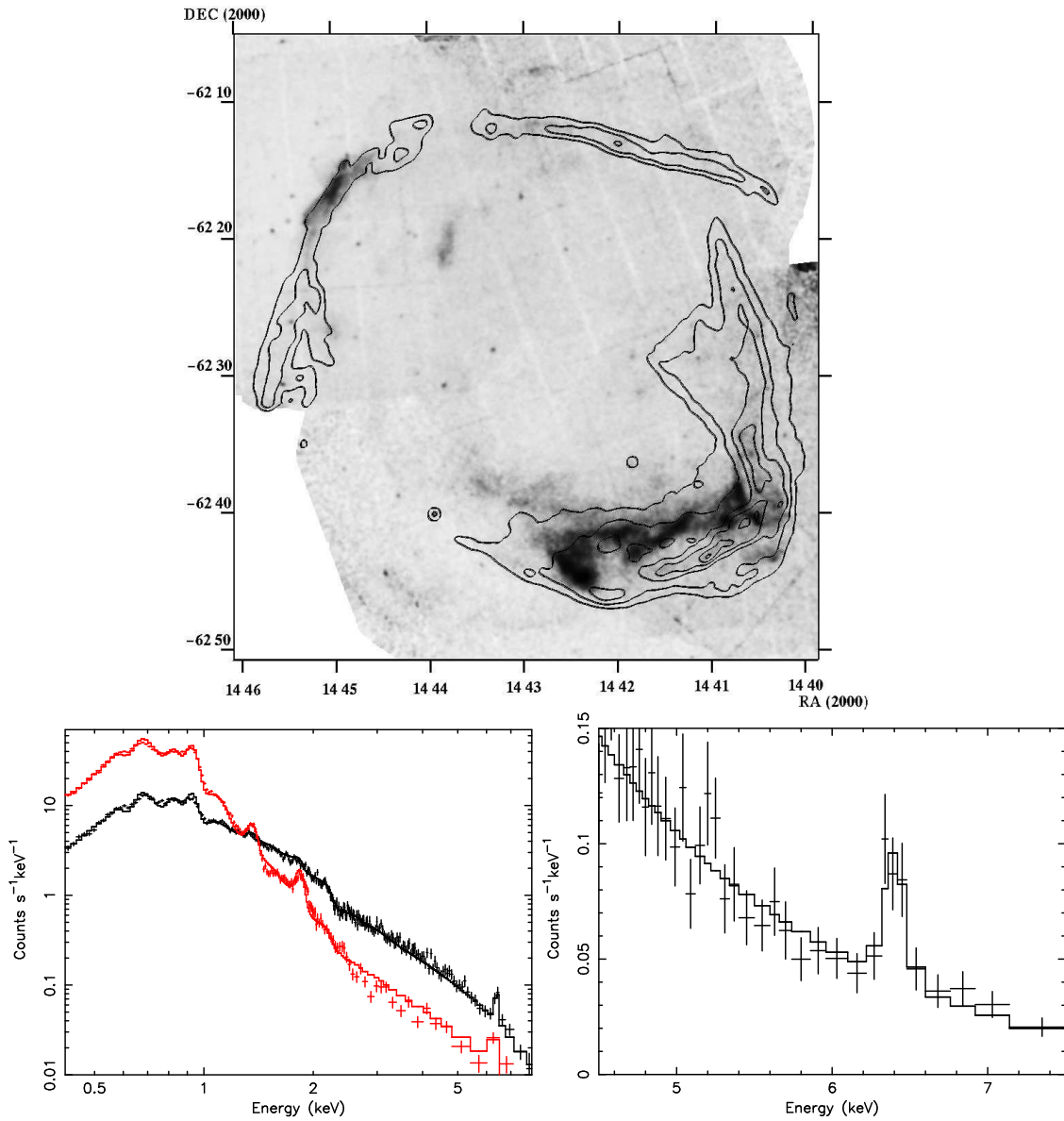


**FIGURE 3.** Left: *XMM-Newton* X-ray mosaic image of RCW 86 in the energy band 1.95-6.8 keV with softer 0.5-1.0 keV emission overlaid as contours. Right, top: Spectra from two distinct regions, one dominated by thermal emission, the other by non-thermal emission. Right, bottom: Detail of the non-thermal spectrum from the Southwest, showing the Fe-K line at 6.4 keV.

## DIFFUSE X-RAY SYNCHROTRON EMISSION: THE CASE OF RCW 86

The X-ray synchrotron emission from the narrow outer rims of Cas A and other young remnants can be understood in the framework of diffusive shock acceleration in combination with synchrotron losses. Ironically, however, the X-ray synchrotron emission

from RX J1713.7-3946, which thanks to observations by *CANGAROO* and *H.E.S.S* may now become an icon of a cosmic ray accelerating SNR [43], seems much more complicated [44].

In many respects RCW 86 (G315.4-2.3) is similar to RX J1713.7-3946; it is a large remnant of  $42'$ , surrounded by molecular clouds observed in CO (Dr. Y. Moriguchi, private communication). Most importantly, its non-thermal X-ray emission is relatively diffuse, but unlike RX J1713.7-3946 there is substantial thermal X-ray emission. The morphology of the thermal X-ray emission is rather different from the non-thermal X-ray emission [7] (Fig. 3). The thermal emission comes from a relatively thin, curving shell, whereas the hard X-ray emission comes predominantly from a slab interior to the southwestern shell, an isolated patch in the the North, and from an isolated patch associated with the northeastern shell.

One puzzling feature of the non-thermal X-ray emission of RCW 86 is the presence of 6.4 keV line emission [7, 45, 8, 9], associated with iron in a low ionization state ( $< \text{Fe XVII}$ , Fig. 3). It was initially proposed that the Fe-K emission pointed to a non-thermal bremsstrahlung of the continuum [7]. In this explanation the continuum and the line emission are caused by the same electrons with energies in the 1-100 keV range. However, a non-thermal electron distribution cannot be maintained for a long time. For that reason it was proposed that the continuum emission is X-ray synchrotron radiation, whereas the Fe-K emission comes from a hot, underionized, pure Fe plasma [46, 8, 9]. The plasma needs to be pure Fe in order to suppress the bremsstrahlung continuum with respect to the line emission. I will adapt here the interpretation that the non-thermal X-ray emission is synchrotron radiation, but I like to point out that an alternative interpretation of the Fe-K emission is fluorescence caused by low energy ( $\sim \text{MeV}$ ) protons. An elaboration on the Fe-K is beyond the present discussion, and will be published elsewhere.

RCW 86 seems to be the result of an explosion in an OB association at a distance of 2.5 kpc [47, 48]. It is therefore likely that the remnant develops in a cavity blown by the hot stars of the OB association [7, 50]. This can explain the curvy nature of the thermal shell, which may be the results of overlapping stellar wind bubbles. In the Southwest the shock seems to run into a molecular cloud with a density of  $n \sim 10 \text{ cm}^{-3}$ .

The shock velocity of RCW 86 has been measured using the  $\text{H}\alpha$  line widths, indicating  $V_s \sim 400 - 800 \text{ km s}^{-1}$  [49]. This is a factor 5 to 10 lower than the shock velocity of remnants like Cas A. It is therefore very surprising that RCW 86 emits X-ray synchrotron emission, as the maximum photon energy for synchrotron radiation is independent of the magnetic field and scales with  $\propto V_s^2$  [44].

Here I discuss preliminary results based on recent *XMM-Newton* and *Chandra* observation of the northeastern shell of RCW 86. The main reason to limit the present discussion to the northeastern part is that at least for that region one can be certain that the forward shock is responsible for the shock acceleration of the X-ray synchrotron emitting electrons, whereas for the other X-ray synchrotron radiating regions either the forward shock is responsible, but the X-ray synchrotron radiation is projected interior to the main shell, or the electrons have been accelerated by the reverse shock [9].



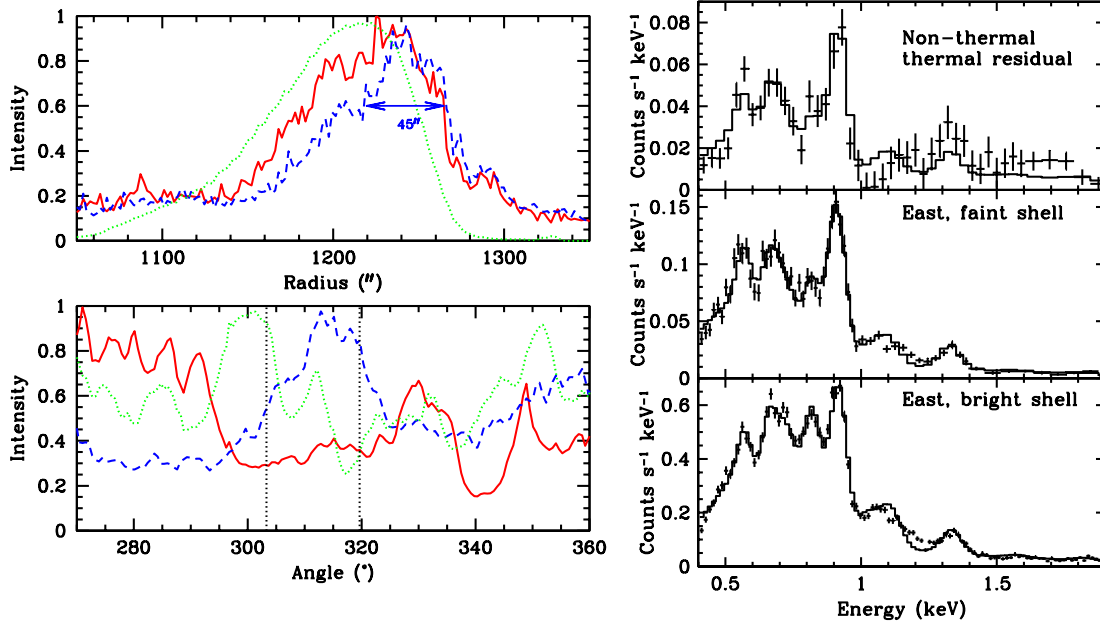


**FIGURE 4.** Right: Intensity profiles of the northeastern part of RCW 86, both in the radial (top) and tangential direction (bottom, from East to North). The 0.5-1 keV X-ray emission is indicated by a red, solid line, the 2-6.8 keV emission by a blue, dashed line and the radio emission [50] by a green, dotted line. Left: Thermal spectra from the eastern shell of RCW 86. The upper panel shows the non-thermal spectrum after subtraction of the best fit power law spectrum. Note the absence of Fe-L emission at  $\sim 0.85$  keV in both the faint outside shell and in the residual thermal emission.

## NON-THERMAL X-RAYS FROM THE NORTHEAST OF RCW 86

Figure 4 shows the emission profiles for the northeastern shell of RCW 86, both for the radial and tangential direction. It is clear from the radial profiles that the X-ray synchrotron emission is more confined to the edge of the shell than the radio and thermal X-ray emission, as is to be expected for the emission from ultra-relativistic electrons accelerated by the forward shock. The typical width of the synchrotron region is  $\sim 45''$  ( $l = 1.7 \times 10^{18}$  cm). Following a similar line of reasoning as for Cas A one can calculate the magnetic field using either the advection (eq. 1) or the diffusion length scale (eq. 3). However, these produce inconsistent answers. For instance, allowing for some uncertainty due to projection effects, one finds for  $V_s = 600 \text{ km s}^{-1}$   $B = 45 - 90 \mu\text{G}$  using the diffusion length scale, but this implies a much smaller advection scale of  $l_a = 9 \times 10^{16}$  cm, violating the requirement for efficient acceleration  $l_d < l_a$  (5). Similarly, using the advection length scale gives  $B = 6 - 13 \mu\text{G}$ , which implies a diffusion length of  $l_d = (1 - 3) \times 10^{19}$  cm, again in violation of (5).

The emission profiles along the shell are also surprising, as the thermal and non-thermal X-ray emission are anti-correlated; the non-thermal emission seems to fill in a gap in the soft X-ray shell. One may think that this points toward locally very efficient cosmic ray acceleration at the cost of heating the plasma. However, one would then

also expect the radio emission to be bright, wherever the non-thermal X-ray emission is bright, but this is clearly not the case (Fig. 4).

Moreover, the thermal emission from this region is very similar to that of the rest of the shell. The thermal emission along the shell shows variation, which is most likely predominantly caused by variations in the ionization parameter  $n_e t$ .<sup>4</sup> The residual thermal emission from the hard X-ray emission is similar to the spectra of other faint regions that have low ionization parameters, i.e.  $n_e t = 4 \times 10^9 \text{ cm}^{-3} \text{ s}$  for  $kT \sim 1 \text{ keV}$ . This suggests that the non-thermal X-ray emission is coming from a region with a low density.

Interestingly, the radio emission from the region with the non-thermal X-ray emission is rather weak, and can only be jointly fitted with a synchrotron model if a flattening of the electron spectrum from -2.2 to 2 is assumed (Fig. 5). This is in agreement with theoretical calculations of cosmic ray spectra that take into account the effect of the cosmic ray pressure on the shock structure [e.g. 51].

So how may the observational facts help to explain the emergence of non-thermal X-ray emission at this particular spot? A solution to this problem may be the large density gradients that are present in SNRs evolving in a cavity blown by stellar winds. Part of the shock may already be plowing through the dense cavity wall, whereas in other regions the shocks still move through the tenuous cavity itself, producing only weak, thermal X-ray emission. As a result, locally, the shock velocity may be substantially higher than  $V_s = 600 \text{ km s}^{-1}$ , as the  $\text{H}\alpha$  measurements are biased toward bright, dense, filaments. Note that for cavity remnants the shock velocity remains high while the shocks move through the cavity, and decelerates rapidly once interacting with the shell [52].

We can estimate the shock velocity and magnetic field strength by demanding that the advection scale and diffusion length scale are equal and consistent with the observed width of the non-thermal X-ray emission of  $\sim 45''$ . This is the case for  $V_s \approx 2700 \text{ km s}^{-1}$ , which would imply  $B \approx 17 \mu\text{G}$ . This is an order of magnitude lower than for Cas A or SN 1006 and helps to explain why the non-thermal X-ray emission is rather diffuse.

Next consider whether such a variation in shock velocity is consistent with the morphology of the northeastern shell, i.e. is the lack of pronounced bulging out of the shell consistent with a locally higher shock velocity? To answer that we need to estimate the time since the brighter parts of the eastern shell started interacting with the cavity wall. For an order of magnitude estimate we can use the diagnostics offered by the thermal spectra, which indicate  $n_e t = 5.4 \times 10^9 \text{ cm}^{-3} \text{ s}$ , whereas the emission measure together with a volume estimate indicates  $n_e \sim 0.5 \text{ cm}^{-3}$ . Together they suggest that the bulk of the plasma was shocked  $\Delta t = 340 \text{ yr}$  ago. Therefore the shock that produces the X-ray synchrotron emission could be as far ahead as  $\Delta r = \Delta V_s \Delta t = 0.7 \text{ pc}$ , corresponding to a fractional difference of  $\Delta r/r = 0.7/16 = 0.04$ , which is very reasonable given RCW 86's morphology.

The idea of substantial local variations in the shock velocity can be best tested by measuring the shock velocity, either from the faint  $\text{H}\alpha$  filaments near the X-ray synchrotron region, or even better, by directly measuring the proper motion of the edge

---

<sup>4</sup> The thermal emission from SNRs is often out of ionization equilibrium. The ionization process scales with the product of electron density and time.

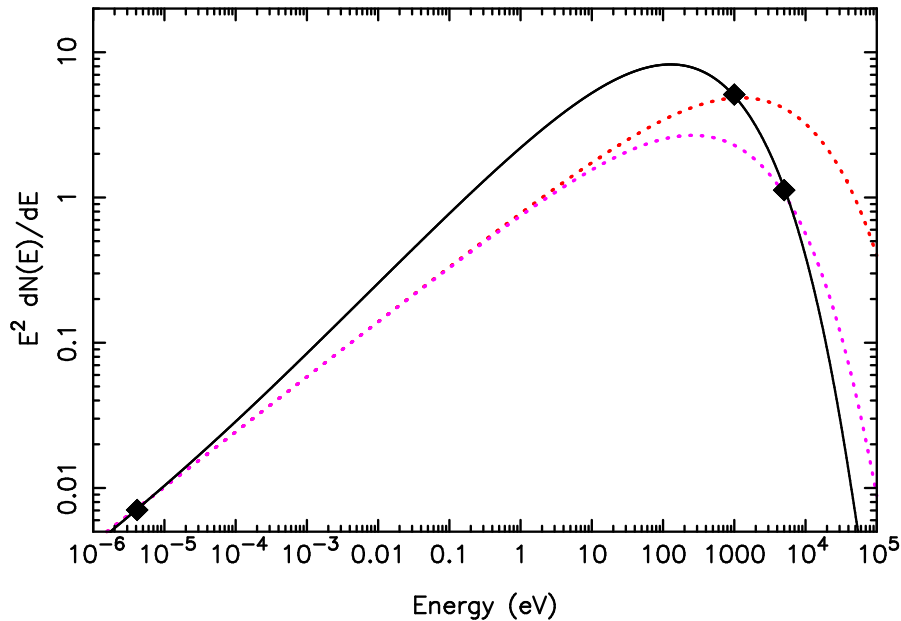


**FIGURE 5.** Synchrotron model for the hard X-ray emitting region in the Northeast. The solid line assumes an electron spectrum that flattens with energy, the colored lines assume a constant power law index (particle index -2.2).

of the non-thermal X-ray emitting region.

## SUMMARY

The discovery of X-ray synchrotron radiation from shell-type supernova remnants has not only provided evidence that supernova remnant shocks are efficient particle accelerators, but has given us a new tool to study the acceleration process. In that respect the high spatial resolution of *Chandra* has been crucial, as it shows that all young Galactic remnants have narrow X-ray synchrotron emitting filaments. The spectra from, and the widths of these filaments indicate that:

- the electron cosmic ray spectrum is loss limited,
- the downstream magnetic fields are relatively high,  $B \geq 0.1$  mG, and consistent with magnetic field amplification by cosmic ray streaming,
- the maximum electron energy is 10 – 40 TeV,
- diffusion takes place at, or close to, the Bohm limit.

The maximum electron energy falls short of the “knee” energy. However, protons are not limited by synchrotron losses. Moreover, the Bohm diffusion and the high magnetic fields makes a maximum proton energy as high as the “knee” plausible, certainly if in the very early phases of these remnants the shock velocities and magnetic fields were higher.

Although the X-ray synchrotron radiation from the narrow filaments of young remnants can be well understood within the framework of diffusive shock acceleration, the more extended X-ray synchrotron radiation from large remnants such as RX J1713.7-3946 and RCW 86 poses some difficulties. I have discussed the X-ray synchrotron emission from a shock region in the Northeast of RCW 86, and I have argued that it can be best understood if the magnetic field is  $B \approx 17 \mu\text{G}$ , and the X-ray synchrotron radiation is comes from region where the shock velocity is considerably faster ( $V_s \approx 2700 \text{ km s}^{-1}$ ) than elsewhere along the shell ( $V_s \approx 600 \text{ km s}^{-1}$ ).

## ACKNOWLEDGMENTS

I would like to thank my collaborators Johan Bleeker, Martin Laming, Peter den Hartog, and Andrei Bykov for their contributions and help, and John Kirk for discussing with me betatron acceleration as a mechanism to enhance X-ray synchrotron emission in Cas A.

## REFERENCES

1. Nagano, M., and Watson, A. A., *Reviews of Modern Physics*, **72**, 689–732 (2000).
2. Koyama, K., et al., *Nat*, **378**, 255–257 (1995).
3. Lazendic, J. S., et al., *ApJ*, **602**, 271–285 (2004).
4. Aharonian, A., et al., *A&A*, **370**, 112–120 (2001).
5. Vink, J., and Laming, J. M., *ApJ*, **584**, 758–769 (2003).
6. Bell, A. R., and Lucek, S. G., *MNRAS*, **321**, 433–438 (2001).
7. Vink, J., Kaastra, J. S., and Bleeker, J. A. M., *A&A*, **328**, 628–633 (1997).
8. Bamba, A., Koyama, K., and Tomida, H., *PASJ*, **52**, 1157–1163 (2000).
9. Rho, J., Dyer, K. K., Borkowski, K. J., and Reynolds, S. P., *ApJ*, **581**, 1116–1131 (2002).
10. Cassam-Chenai, G., et al., in *IAU Symposium*, 2004, pp. 73.
11. Bamba, A., Ueno, M., Nakajima, H., and Koyama, K., *ApJ*, **602**, 257–263 (2004).
12. Smith, D. A., and Wang, Q. D., *ApJ*, in press (2004).
13. Stephenson, F. R., and Green, D. A., *Historical supernovae and their remnants*, Oxford: Clarendon Press, 2002.
14. Thorstensen, J. R., Fesen, R. A., and van den Bergh, S., *AJ*, **122**, 297–307 (2001).
15. Vink, J., Bloemen, H., Kaastra, J. S., and Bleeker, J. A. M., *A&A*, **339**, 201–207 (1998).
16. Delaney, T., and Rudnick, L., *ApJ*, **589**, 818 (2003).
17. Reed, J. E., Hester, J. J., Fabian, A. C., and Winkler, P. F., *ApJ*, **440**, 706–721 (1995).
18. The, L.-S., et al., *A&AS*, **120**, C357+ (1996).
19. Favata, F., et al., *A&A*, **324**, L49–L52 (1997).
20. Allen, G. E., et al., *ApJL*, **487**, L97–L100 (1997).
21. Bleeker, J. A. M., et al., *A&A*, **365**, L225–L230 (2001).
22. Gotthelf, E. V., et al., *ApJL*, **552**, L39–L43 (2001).
23. Hwang, U., et al., *ApJL*, in press (2004).
24. Berezhko, E. G., and Völk, H. J., *A&A*, **419**, L27–L30 (2004).
25. Bamba, A., Yamazaki, R., Ueno, M., and Koyama, K., *ApJ*, **589**, 827–837 (2003).
26. Hwang, U., Decourchelle, A., Holt, S. S., and Petre, R., *ApJ*, **581**, 1101–1115 (2002).
27. Cassam-Chenai, G., et al., *A&A*, **414**, 545–558 (2004).
28. Yamazaki, R., Yoshida, T., Terasawa, T., Bamba, A., and Koyama, K., *A&A*, **416**, 595–602 (2004).
29. Berezhko, E. G., Ksenofontov, L. T., and Völk, H. J., *A&A*, **412**, L11–L14 (2003).
30. Willingale, R., West, R. G., Pye, J. P., and Stewart, G. C., *MNRAS*, **278**, 749–762 (1996).
31. Rothenflug, R., et al., *A&A*, **425**, 121–131 (2004).
32. Vink, J., *Adv. of Space Research*, **33**, 356–365 (2004).

33. Vink, J., et al., *ApJL*, **560**, L79–L82 (2001).
34. Vink, J., et al., *A&A*, **344**, 289–294 (1999).
35. Hughes, J. P., Rakowski, C. E., Burrows, D. N., and Slane, P. O., *ApJL*, **528**, L109–L113 (2000).
36. DeLaney, T., et al., *ApJ*, in press (2004).
37. Anderson, M. C., and Rudnick, L., *ApJ*, **441**, 307–333 (1995).
38. Laming, J. M., *ApJ*, **546**, 1149–1158 (2001).
39. Laming, J. M., *ApJ*, **563**, 828–841 (2001).
40. Lyutikov, M., and Pohl, M., *ApJ*, **609**, 785–796 (2004).
41. Kirk, J. G., “Particle Acceleration,” in *Saas-Fee Advanced Course 24: Plasma Astrophysics*, 1994, pp. 225–314.
42. Wright, M., Dickel, J., Koralesky, B., and Rudnick, L., *ApJ*, **518**, 284–297 (1999).
43. Enomoto, R., et al., *Nat*, **416**, 823–826 (2002).
44. Uchiyama, Y., Aharonian, F. A., and Takahashi, T., *A&A*, **400**, 567–574 (2003).
45. Bocchino, F., Vink, J., Favata, F., Maggio, A., and Sciortino, S., *A&A*, **360**, 671–682 (2000).
46. Borkowski, K. J., Rho, J., Reynolds, S. P., and Dyer, K. K., *ApJ*, **550**, 334–345 (2001).
47. Westerlund, B. E., *AJ*, **74**, 879–881 (1969).
48. Rosado, M., Le Coarer, E., and Georgelin, Y. P., *A&A*, **286**, 231–242 (1994).
49. Ghavamian, P., Raymond, J., Smith, R. C., and Hartigan, P., *ApJ*, **547**, 995–1009 (2001).
50. Dickel, J. R., Strom, R. G., and Milne, D. K., *ApJ*, **546**, 447–454 (2001).
51. Ellison, D. C., and Reynolds, S. P., *ApJ*, **382**, 242–254 (1991).
52. Tenorio-Tagle, G., Rozyczka, M., Franco, J., and Bodenheimer, P., *MNRAS*, **251**, 318–329 (1991).